JES
JOURNAL OF ENVIRONMENTAL SCIENCES
ISSN 1001-0742
CN 11-2629/X
February 1, 2014 Volume 26 Number 2
www.jesc.ac.cn

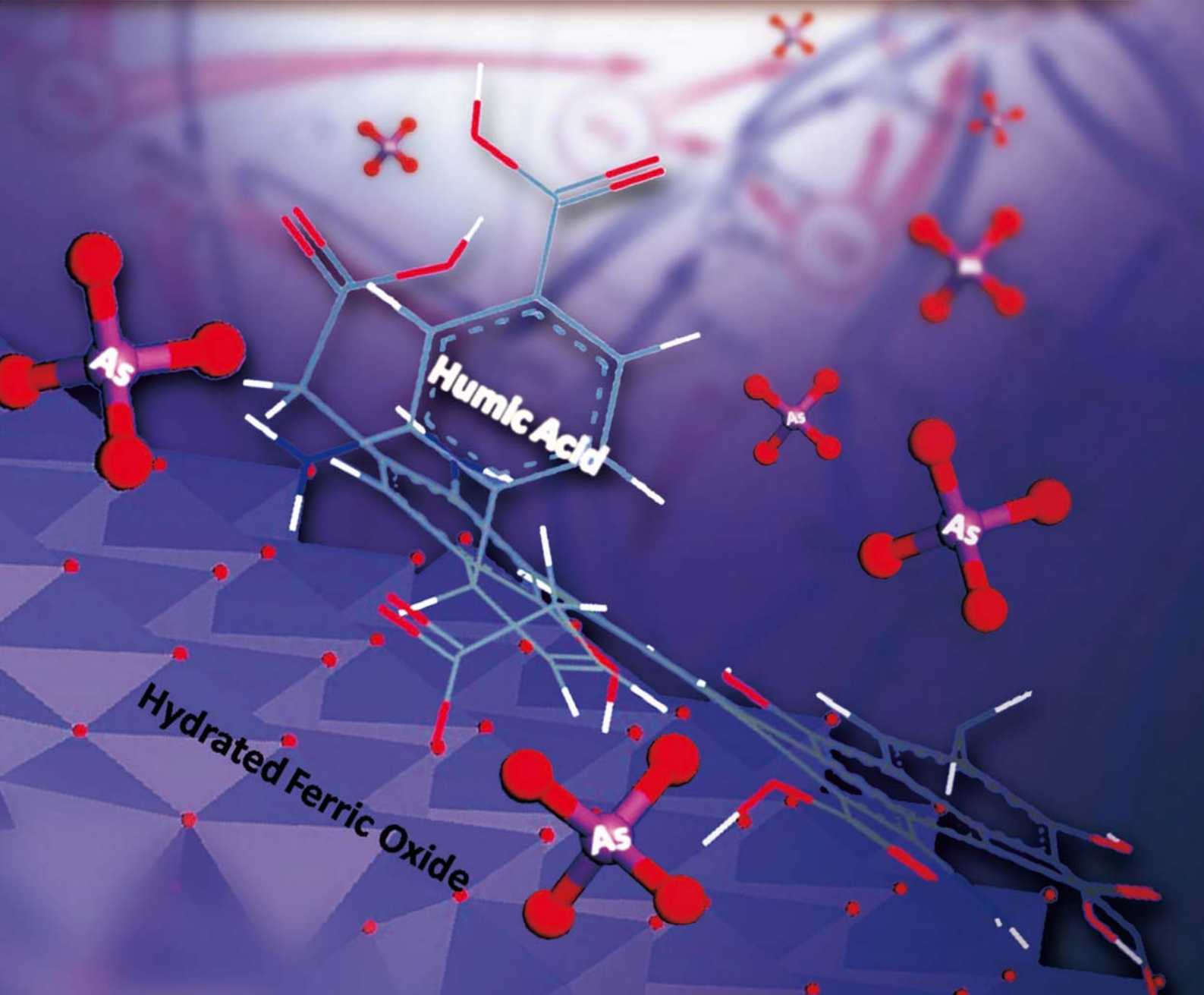

ELSEVIER
Science Press
Sponsored by
Research Center for Eco-Environmental Sciences
Chinese Academy of Sciences

ISSN 1001–0742 **Journal of Environmental Sciences** Vol. 26 No. 2 2014

CONTENTS

Aquatic environment

Atmospheric environment

Environmental health and toxicology

Environmental catalysis and materials

Serial parameter: CN 11-2629/X*1989*m*261*en*P*30*2014-2

Journal of Environmental Sciences 26 (2014) 483–491

Available online at www.sciencedirect.com

Journal of Environmental Sciences

www.jesc.ac.cn

Debromination of decabromodiphenyl ether by organo-montmorillonite-supported nanoscale zero-valent iron: Preparation, characterization and influence factors

Zhihua Pang[1,2], Mengyue Yan[2], Xiaoshan Jia[1,*], Zhenxing Wang[2], Jianyu Chen[2]

1. School of Environmental Science and Engineering, Sun Yat-Sen University, Guangzhou 510630, China. E-mail: Pangzhihua08@gmail.com
2. South China Institute of Environmental Sciences, Ministry of Environmental Protection, Guangzhou 510655, China

ARTICLE INFO

Article history:
Received 19 March 2013
revised 15 May 2013
accepted 22 May 2013

Keywords:
supported nanoscale zero-valent iron
organo-montmorillonite
decabromodiphenyl ether (BDE-209)
degradation
influence factors
DOI: 10.1016/S1001-0742(13)60419-2

ABSTRACT

An organo-montmorillonite-supported nanoscale zero-valent iron material (M-NZVI) was synthesized to degrade decabromodiphenyl ether (BDE-209). The results showed that nanoscale zero-valent iron had good dispersion on organo-montmorillonite and was present as a core-shell structure with a particle size range of nanoscale iron between 30–90 nm, characterized by XRD, SEM, TEM, XRF, ICP-AES, and XPS. The results of the degradation of BDE-209 by M-NZVI showed that the efficiency of M-NZVI in removing BDE-209 was much higher than that of NZVI. The efficiency of M-NZVI in removing BDE-209 decreased as the pH and the initial dissolved oxygen content of the reaction solution increased, but increased as the proportion of water in the reaction solution increased.

Introduction

Due to its advantages of large specific surface area, good reactivity, strong reducing power and low cost, nanoscale zero-valent iron (NZVI) has recently attracted great interest (Li et al., 2006; Crane and Scott, 2012; Chen et al., 2011a). It can be used widely in the remediation and degradation of various kinds of pollutants, especially halogenated organic pollutants, such as nitrobenzene compounds (Dong et al., 2010), polychlorinated biphenyls (PCBs) (Lowry and Johnson, 2004), polybrominated diphenyl ethers (PBDEs) (Shih and Tai, 2010), and dioxins (Kim et al., 2008). However, as NZVI tends to aggregate (Sun et al., 2006; Zhan et al., 2008) and is easily oxidized to form an oxide layer on the surface of particles in the air (Liu and Lowry, 2006), both of which reduce the activity and efficiency of nanoscale zero-valent iron. By immobilizing or supporting NZVI on a solid material it is feasible to overcome its easy aggregation, easy oxidation and poor dispersion. In recent years, a number of materials, such as activated carbon (Xu et al., 2010), zeolite (Lee et al., 2007), porous silica (Qiu et al., 2011), and kaolin (Zhang et al., 2011a), have been used as carriers for NZVI, and these composites show great performance in the degradation of various kinds of pollutants.

Montmorillonite is a kind of clay mineral with a layered structure, high surface area and strong adsorption characteristics (Schoonheydt, 2002). Also, montmorillonite can be used as a good carrier and dispersant, to support NZVI prepared by a liquid phase reduction reaction (Fang et al., 2010). This composite was found to effectively remove a variety of organic pollutants, such as nitrobenzene compounds (Gu et al., 2010), methyl orange (Chen et al.,

* Corresponding author. E-mail: eesjxs@mail.sysu.edu.cn

2011b), atrazine (Zhang et al., 2011b) and chlorophenols (Dorathi and Kandasamy, 2012). In addition, montmorillonite can be modified by surface-active agents (such as cetyl trimethyl ammonium bromide) through cation exchange to form organo-montmorillonite, which is hydrophobic instead of hydrophilic and therefore has high adsorption capacity for hydrophobic organic pollutants. Moreover, organo-montmorillonite can be used to support and disperse NZVI, and the prepared new composite materials can effectively degrade hydrophobic organic contaminants, such as pentachlorophenol (Li et al., 2011) and catechol tannin (Shakir et al., 2008).

PBDEs widely used in electronic, chemical, electrical, textile, and other industries as a typical kind of brominated flame retardants (Luo et al., 2009), are ubiquitous in the environment, with high hydrophobicity, persistence, bioaccumulation and toxicity (Law et al., 2006), among which decabromodiphenyl ether (BDE-209) is the only one that is still in production and large-scale use. There are many techniques to remove BDE-209, such as biological degradation (He et al., 2006), photocatalytic degradation (An et al., 2008) and zero-valent iron reduction. In particular, zero-valent iron reduction technology has gained great interest due to its high efficiency and low cost in the degradation of PBDEs. The use of zero-valent iron in the degradation of PBDEs was carried out by Keum and Li (2005) for the first time. Subsequently, nanoscale zero-valent iron was synthesized to degrade PBDEs (Qiu et al., 2011; Fang et al., 2011a, 2011b; Zhuang et al., 2010, 2011; Li et al., 2007), and showed high degradation efficiency, and Yu et al. studied the debromination of BDE-209 by a montmorillonite-clay-supported nanoscale iron material (Yu et al., 2012). However, there are still few studies about the use of organo-montmorillonite-supported nanoscale zero-valent iron in the degradation of BDE-209.

In this study, a supported nanoscale zero-valent iron material was prepared by a liquid phase reduction method with organo-montmorillonite as carrier and dispersant. Then, characterization was conducted by various means, such as XRD, BET, SEM, TEM, EDS, XPS, XRF, and ICP-AES. Finally, various factors influencing its degradation of BDE-209 were studied, including the pH, the initial dissolved oxygen content and the proportion of solvents.

1 Materials and methods

1.1 Chemicals

Sodium-montmorillonite, with a purity of montmorillonite of 95%, was purchased from Anji County, Zhejiang Province, China; its cation exchange capacity (CEC) was 112.0 mmol/100g. Decabromodiphenyl ether (BDE-209) standard solution was purchased from Accustandard Company and used to establish a standard curve. Chemical grade BDE-209 (pure type, solid, 99%) was purchased from Shanghai ANPEL Scientific Instrument Co., Ltd. (Shanghai, China) and used in the degradation tests. Methanol (HPLC grade) was purchased from Shanghai ANPEL Scientific Instrument Co., Ltd. (Shanghai, China). Other reagents such as cetyl trimethyl ammonium bromide (CTMAB), tetrahydrofuran (THF), ferrous sulfate heptahydrate, sodium borohydride, anhydrous ethanol, nitric acid, sodium bromide and sodium hydroxide were all of analytical purity, purchased from Guangzhou Chemicals Co., Ltd. (Guangzhou, China). The experimental water was self-made deionized deoxygenated pure water.

1.2 Preparation of materials

1.2.1 Preparation of organic-modified montmorillonite

The sodium-montmorillonite was organically modified mainly through an ion exchange process (Lowry et al., 2004; Zhu et al., 1997). A group of preliminary experiments were carried out to determine the optimum amount of modifier. The specific method was as follows: 5.0 g of sodium-montmorillonite (named MT) was added into a conical flask containing 200 mL deionized water, then 2.04 g cetyltrimethylammonium bromide (CTMAB) was added. After two hours of reaction with stirring at 60°C the modified product was centrifuged and washed several times, then dried at 70°C for 12 hr. The ground products were screened through a 100 mesh sieve, and finally activated at 115°C for 2 hr. The obtained organo-montmorillonite was named CMT.

1.2.2 Preparation of organo-montmorillonite supported nanoscale zero-valent iron

Organo-montmorillonite-supported nanoscale zero-valent iron was prepared mainly by a liquid phase reduction method of $FeSO_4$ and $NaBH_4$ according to the literature, (Fang et al., 2010; Shahwan et al., 2010) with some modification. The specific method was as follows: 5.0 g organo-montmorillonite was added into a beaker containing 200 mL deionized deoxygenated water, and a certain amount (m_{CMT}/m_{Fe} = 4:1) of $FeSO_4{\cdot}7H_2O$ was added. A volume of 100 mL newly prepared $NaBH_4$ solution was added dropwise to yield a B/Fe molar ratio of 3:1 and stirred for 9 hr at room temperature. Then the product was separated by filtration and washed with alcohol three times, vacuum dried for 12 hr at 60°C and named M-NZVI. Also, nanoscale iron particles were prepared in the same way without participation of organo-montmorillonite in the reaction process, and the product was named NZVI.

1.3 Characterization of the materials

The BET surface area of the material was analyzed with an ASAP2020 system (Quantachrome Instruments Inc., USA).

The identification of crystalline phases of nanomaterials

was conducted by X-ray diffraction (XRD, Bruker D8 Advance, Cu target, $K\alpha$ radiation, 40 kV, 40 mA, Germany).

The particle size, morphology and structure of the material were characterized by scanning election microscopy (SEM) (LEO 1530 VP, Germany) and transmission electron microscopy (TEM) (Technai G2 F20, FEI Company, USA). The elemental composition of the synthetic nanomaterials was measured by the TEM's self-contained enery-dispersive X-ray spectroscopy (EDS) spectrometer.

The surface valence of nanomaterials was analyzed by X-ray photoelectron spectroscopy (XPS, British Kratos Company, AXIS Ultra). An aluminum target X-ray source (Al, $K\alpha$, $h\nu$ = 1486.7 eV) with monochromator was used in the XPS instrument.

The surface composition of nanomaterials was measured by an X-ray fluorescence spectrometer (XRF, S2 Ranger, Bruker, Germany) equipped with a Pd target X-ray tube (maximum power of 50 W), 9-bit auto optical filter switch and X Flash silicon drift detection device. The sample was filled into a mold at first when measured, and then compacted with a tablet press for 3 min, and finally tested on the machine.

The major elemental contents in bulk nanomaterials were analyzed by inductively coupled plasma atomic emission spectroscopy (ICP-AES, Leeman Company, Profile SPEC, USA) after being dissolved in concentrated hydrochloric acid.

1.4 Experimental process

1.4.1 Preparation of BDE-209 solution

First, a stock solution of BDE-209 (500 mg/L) was prepared with tetrahydrofuran (THF) according to the literature (Zhao et al., 2009). Briefly, 0.01 g BDE-209 solid was dissolved in a brown conical flask containing 200 mL THF and stirred at 200 r/min for 48 hr. Then, the reaction solution was obtained directly by diluting the stock solution with a THF-water mixture (THF:water = 7:3 (*V/V*)).

1.4.2 Process of batch experiment

First, 50 mL BDE-209 mixed solution (2.0 mg/L) was added into a 100 mL conical flask with a stopper used as a reactor, and the synthetic material was added. The reactor was then sealed and stirred with rotating speed controlled at 150 r/min at (25±1)°C. Sampling was conducted at specified time intervals; samples were filtered, and the filtrate was used for analysis of the concentration of BDE-209. All samples were performed in four replications.

1.5 Analytical method

The concentration of BDE-209 was measured by HPLC (Shimadzu LC-20AT) equipped with a SupelcosilTMK C18 chromatographic column (250 mm × 4.6 mm, 5 μm) and detected by UV spectrophotometry at a wavelength of 204 nm and 226 nm in the mobile phase (1.0 mL/min) composed of acetonitrile/water = 98/2 (*V/V*).

The concentration of bromide ion was determined by an ion selective electrode with a Leici PHS-3C instrument equipped with a 301 bromide ion selective electrode and 801 double-liquid-junction saturated calomel electrode.

The concentration of iron ions in the solution was determined with an Atomic Absorption Spectrometer (Shimadzu AA-7000, Japan).

2 Results and discussion

2.1 Characterization of materials

2.1.1 BET analysis

Specific surface area is the main indicator reflecting the adsorption capacity of synthetic adsorbents. The specific surface area of M-NZVI was 36.431 m^2/g, which was larger than that of NZVI (26.875 m^2/g) and that of CMT (18.384 m^2/g) (**Table 1**). The result was similar to surface areas of other supported nanoscale iron materials (Zhang et al., 2011a). Compared with CMT, the specific surface area of M-NZVI increased significantly, which was attributed to the large number of the iron particles supported on the surface or interlayers of organo-montmorillonite. In addition, the pore volume of CMT, NZVI, and M-NZVI was 0.195, 0.106, and 0.162 cm^3/g, respectively. The porosity of M-NZVI was reduced slightly compared with that of CMT, which might be caused by clogging of pores by the iron nanoparticles.

2.1.2 XRD analysis

The wide-angle and narrow-angle XRD patterns of CMT, NZVI, and M-NZVI are shown in **Fig. 1**. There was an obvious characteristic diffraction peak of α-Fe appearing at 2θ = 44.78° for both NZVI and M-NZVI (Sun et al., 2006; Fang et al., 2010, 2011a; Li et al., 2011), indicating that the zero-valent iron had been supported successfully on organo-montmorillonite. In addition, a weaker impurity peak of iron oxide (2θ = 35.85°) was found in the XRD pattern of M-NZVI, indicating that the iron nanoparticles supported on the surface of organo-montmorillonite had a core-shell structure, with an inner core of α-Fe and iron oxide coated as a shell on the surface (Sun et al., 2006; Fang et al., 2010). The peak at 44.78° of M-NZVI was weaker and broader compared with that of

Table 1 Summary of surface properties

Sample name	BET surface area (m^2/g)	Pore volume (m^2/g)	Average pore diameter (nm)
CMT	18.384	0.195	30.366
NZVI	26.875	0.106	26.436
M-NZVI	36.431	0.162	24.963

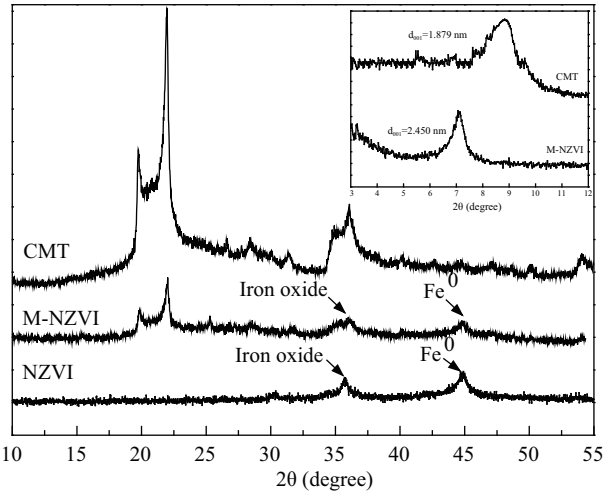

Fig. 1 X-ray diffraction patterns of CMT; M-NZVI; and NZVI.

NZVI, indicating that the particle size of iron nanoparticles supported on organo-montmorillonite was much smaller than that of NZVI.

Based on narrow-angle XRD patterns of NZVI and M-NZVI, the basal spacing d_{001} of M-NZVI was 2.450 nm as calculated with the Bragg equation, which was 0.571 nm larger than the basal spacing of CMT (d_{001} = 1.879 nm). In addition, the characteristic peak of M-NZVI shifted toward lower angle, indicating that nano-iron particles had been successfully inserted into the interlayers of montmorillonite. The formed ZVI clusters were intercalated between the layers and acted as pillars, thus expanding the interlayer distance. Meanwhile, there were few iron ions found in the solution after the reaction, which indicated that iron ions were almost completely loaded onto the organo-montmorillonite.

2.1.3 SEM analysis

The morphology and particle distribution of CMT, NZVI, and M-NZVI were analyzed by SEM (**Fig. 2**). The organo-montmorillonite had a layered structure, and there were a lot of crevices between different layers, which provided enough space for supporting nanoscale iron particles. NZVI particles were aggregated as chain-like clusters, while nanoscale iron particles in M-NZVI were evenly distributed on the entire surface and edges of the organo-montmorillonite. The nanoscale iron particles in M-NZVI were spherical, with particle size of 30–90 nm. This showed that immobilizing iron nanoparticles on a porous material was an effective method of preventing iron nanoparticles from aggregating (Sun et al., 2006; Qiu et al., 2011; Fang et al., 2010; Li et al., 2011; Shi et al., 2011; Jia et al., 2012).

The particle sizes of nano-iron grains near the edges of crevices and interlayers were smaller than those on the surface of montmorillonite and ranged from 5–40 nm as shown in **Fig. 2e**. As it was difficult to characterize the particle size within the layers by SEM and TEM, this could only be done by analyzing the XRD results. From the above-mentioned data, the basal spacing d_{001} of M-NZVI was 2.45 nm. Minus the thickness of a single layer of montmorillonite (0.92 nm), the interlayer spacing could be calculated as 1.53 nm, meaning that the nano-iron grain diameter between the layers was less than 1.53 nm.

2.1.4 TEM analysis

The TEM images of NZVI and M-NZVI are shown in **Fig. 3**. Although the particle size of NZVI particles was less than 100 nm, most of the nanoscale iron particles aggregated into chains, while excellent dispersion of the iron nanoparticles was achieved in M-NZVI. The core-shell structure of M-NZVI is clearly shown in **Fig. 3c,**

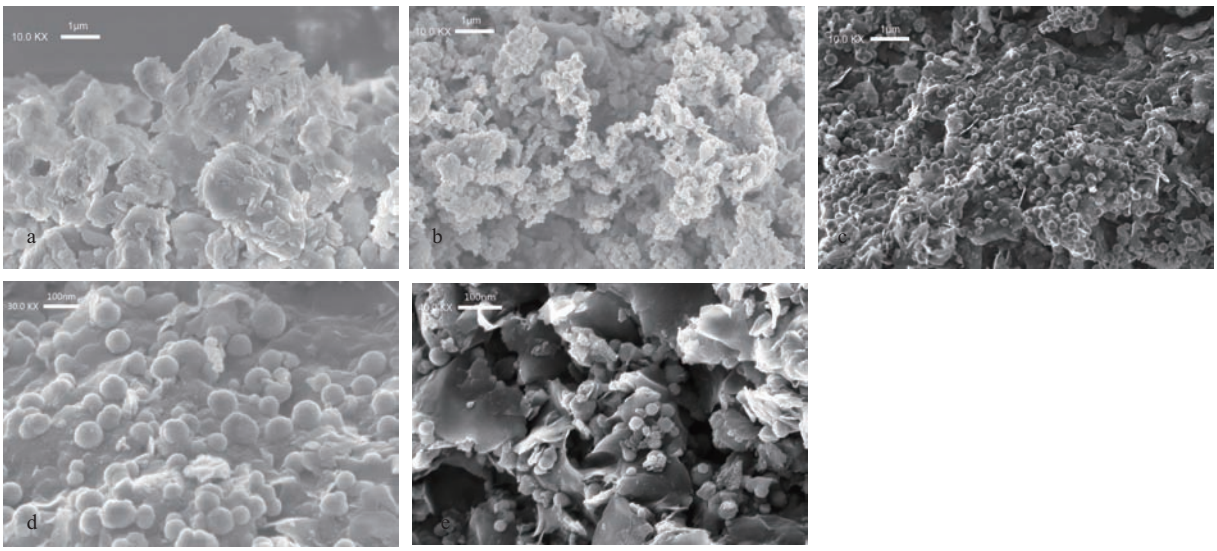

Fig. 2 SEM images. (a) CMT; (b) NZVI; (c) M-NZVI (10.0 KX); (d) M-NZVI (30.0 KX); (e) M-NZVI (40.0 KX).

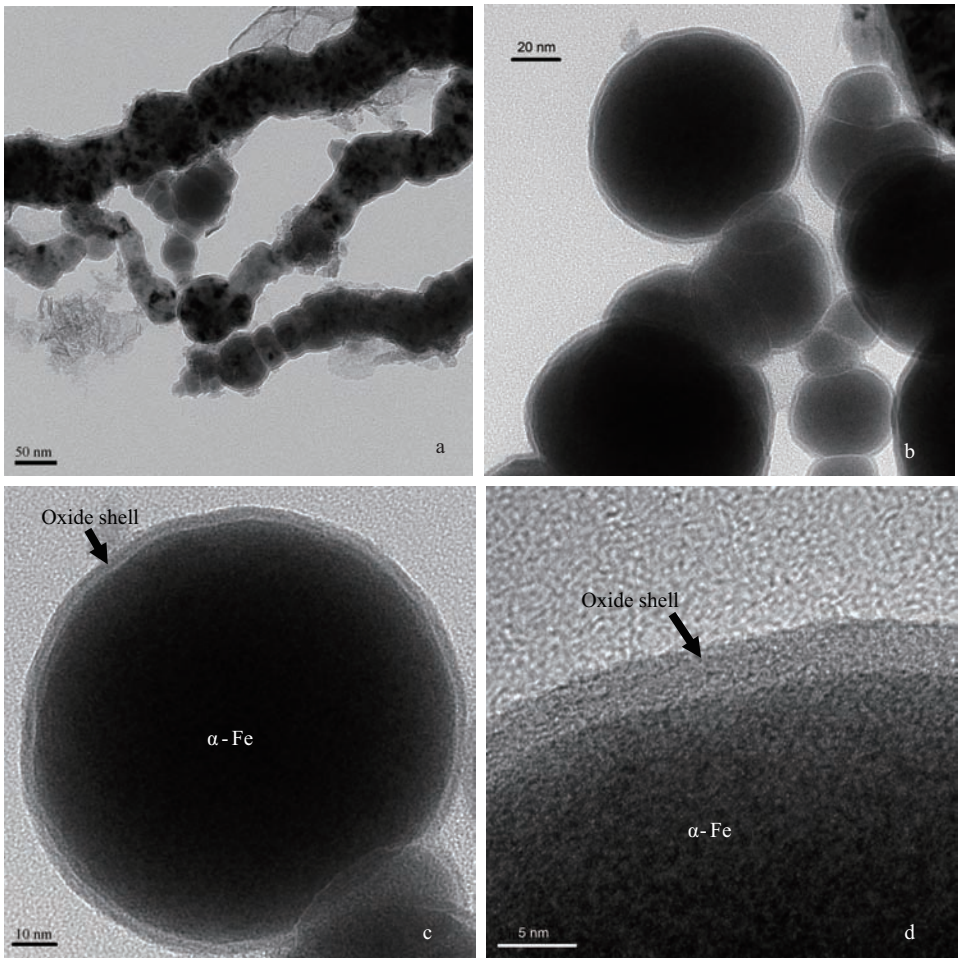

Fig. 3 TEM images of NZVI (a) and M-NZVI (b, c, d).

d. The thickness of the shell was measured at about 2.5–4.0 nm, and the results were similar with other works (Kim et al., 2008; Fang et al., 2010; Shi et al., 2011; Martin et al., 2008; Üzüm et al., 2008). According to Caberra-Mott theory (Fang et al., 2010), it would take 600 years for the iron oxide shell to increase the thickness by 1.0 nm. Therefore, the M-NZVI materials had a core-shell structure with strong oxidation resistance that would remain stable under common temperature and pressure conditions.

2.1.5 XPS analysis

The surface composition of M-NZVI was analyzed by XPS (**Fig. 4**). The binding energy of the characteristic Fe ($2p_{3/2}$) photoelectron peak was 710.73 eV, similar to that of α-Fe_2O_3 (Fang et al., 2011a), indicating that a layer of iron oxide covered the surface of the nanoscale iron particles (Sun et al., 2006; Gu et al., 2010). The characteristic Fe ($2p_{3/2}$) peak of M-NZVI after the reaction was at 711.15 eV, similar to the binding energy of FeOOH (Qiu et al., 2011; Martin et al., 2008; Üzüm et al., 2009), suggesting that precipitated hydroxide could be formed on M-NZVI after hydrolysis and adsorption (Üzüm et al., 2008), and there could be a variety of iron oxides (such as α-Fe_2O_3, FeOOH) (Kanel et al., 2005; Li and Zhang, 2006) on the surface. In addition, a smaller characteristic peak was found near the binding energy of 706.30 eV, corresponding to zero-valent iron (Sun et al., 2006). As a layer of iron oxide of 3–5 nm encapsulated the surface of the iron particles, it was difficult for the X-rays to penetrate into the iron core.

2.1.6 Component analysis

To clarify the composition of the M-NZVI samples, EDS, XRF, and ICP-AES were adopted for analysis. The results are shown in **Table 2** and **Fig. 5**. There was considerable difference among the results of the three methods, because EDS and XRF mainly determine the surface composition of a material, while ICP-AES determines the bulk composition. ICP-AES results showed that the iron content of the material was as high as 85.3%, which was much higher than the results of EDS and XRF, while the EDS result showed that oxygen was present at a high percentage, indicating that the surface of NZVI had been oxidized. The iron content in M-NZVI measured by ICP-AES was 15.6%, which agreed well with the mass ratio of

Table 2 Elemental composition of the materials

Type	EDS results (wt.%)	XRF results (wt.%)	ICP-AES results (wt.%)
CMT	Si 39.9	Si 36.9	
	O 46.6	Mg 4.6	/
	Other elements 13.5	Other elements 58.5	
NZVI	Fe 63.4	Fe 59.1	Fe 85.3
	O 32.8	Other elements 40.9	Other elements 14.7
	Other elements 4.8		
M-NZVI(before reaction)	Fe 35.9	Fe 29.1	Fe 15.6
	Si 26.4	Si 20.8	Si 39.1
	O 29.2	Other elements 50.1	Other elements 45.3
	Other elements 8.5		
M-NZVI(after reaction)	Fe 32.7	Fe 27.6	Fe 12.4
	Si 25.8	Si 20.6	Si 38.5
	O 31.4	Other elements 51.8	Other elements 49.1
	Other elements 10.1		

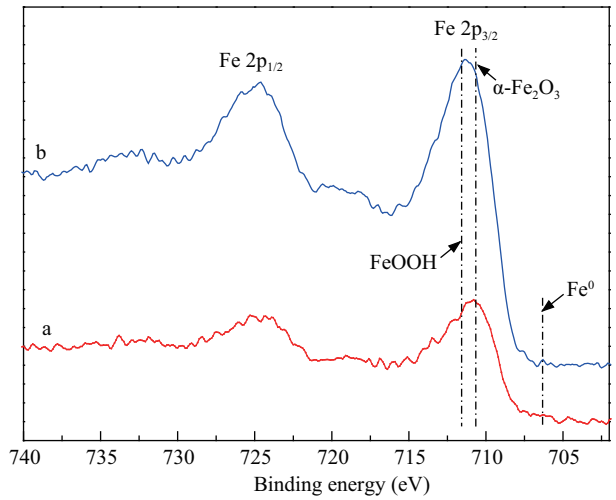

Fig. 4 XPS spectrum for the narrow scan of Fe 2p. Line a: narrow scan of Fe 2p before reaction; line b: narrow scan of Fe 2p after reaction.

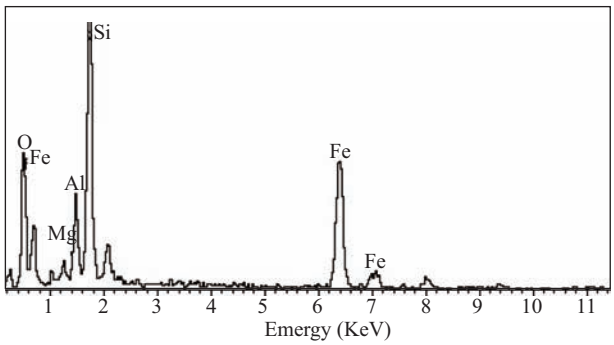

Fig. 5 A typical EDS spectrum of M-NZVI.

montmorillonite/iron of 4:1 determined by the preparation of the material. In addition, the iron content of M-NZVI after the reaction was lower than that before the reaction (Xu et al., 2010), while the oxygen content in the material was higher, indicating that iron oxides precipitated on the surface.

2.2 Results of analysis on influencing factors

2.2.1 Influence of different materials

Four types of materials (MT, CMT, NZVI, and M-NZVI) were used to compare the removal efficiency of BDE-209 (**Fig. 6a**). The removal efficiency of BDE-209 by MT, CMT, NZVI, and M-NZVI after 24 hr was 5.65%, 71.45%, 24.64%, and 98.02%, respectively. This showed that CTMAB was effective in enhancing the adsorption ability of strongly hydrophobic halogenated organic pollutants on CMT by changing the montmorillonite surface from hydrophilic to hydrophobic. Although NZVI could degrade halogenated organic pollutants, it was not effective for the degradation for BDE-209 due to its easy aggregation and oxidation by air in the natural environment. Compared with NZVI, the removal efficiency of M-NZVI for BDE-209 was up to 98.02%, which was about three times higher than that of NZVI. The main reasons were that organo-montmorillonite possessed large specific surface area and could effectively adsorb BDE-209, and that zero-valent iron could be fully dispersed in the organo-montmorillonite thus reducing its aggregation, as confirmed by SEM and TEM. This could be greatly beneficial for the reaction between nanoscale zero-valent iron and BDE-209 in aqueous solution. Similar results were also obtained by others (Zhang et al., 2011a, b; Chen et al., 2011b; Li et al., 2011; Fang et al., 2011a). The high adsorption ability of organo-montmorillonite would also enhance the degradation of BDE-209 by nanoscale zero-valent iron (Li et al., 2011a).

The bromide ion concentration was also measured during the degradation. As seen from **Fig. 6b**, the release rate of bromide ion by M-NZVI could be up to 17.41%, while release of bromide ion by NZVI, CMT, and MT was only 4.82%, 1.83%, and 2.02%, respectively. In addition to M-NZVI, only NZVI caused significant debromination, while

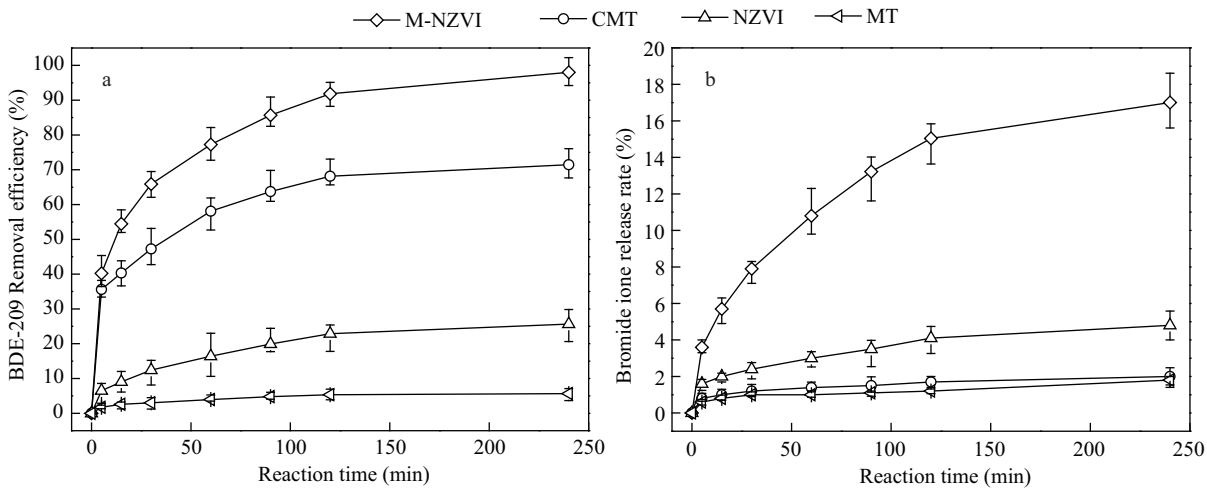

Fig. 6 Effect of different materials on BDE-209 removal (a) and bromide ion release rate of different materials (b). Experimental conditions: initial BDE-209 concentration 2.0 mg/L; material dosage 0.60 g; initial pH 5.5; temperature (25 ± 1) °C.

CMT and MT materials had little debromination ability. This indicated that adsorption was the main process for the removal of BDE-209 by CMT.

It can be also seen from **Fig. 6** that the degradation rate of M-NZVI was relatively fast in the initial 30 min, and then slowed down gradually. This is because nanoscale zero-valent iron on the M-NZVI would be gradually oxidized and form a layer of oxide or hydroxide on its surface as the reaction proceeds, resulting in a continuous covering on the reaction sites of the M-NZVI, leading to the reduction of the removal efficiency for BDE-209 (Fang et al., 2011b).

2.2.2 Influence of initial pH, dissolved oxygen in reaction solution, different proportions of co-solvents

As hydrogen atoms were required for the degradation of halogenated organic pollutants by nanoscale zero-valent iron, the pH should be of great influence on the process (Zhang et al., 2009, 2011; Shih et al., 2009). Four initial pH values (3.0, 5.5, 7.0, and 9.0) were used for the degradation of BDE-209. As seen from **Fig. 7a**, the removal efficiency of M-NZVI for BDE-209 decreased with the increase of pH, which was consistent with the results of Li et al. (2011). In neutral (pH 7.0) and alkaline (pH 9.0) conditions, the removal efficiency of BDE-209 was 76.04% and 65.90%, respectively, while the removal efficiency for BDE-209 at pH 5.5 and 3.0 was 98.25% and 100.0%, respectively. This showed that acid conditions could be more favorable for the debromination of BDE-209, due to more active hydrogen atoms being produced by M-NZVI. Also, hydrogen ion could promote the dissolution of the thin layer of oxide on the surface of M-NZVI (Shih et al., 2010; Zhang et al., 2009), and prevent the precipitation of iron oxide and hydroxide (He et al., 2012).

2.2.3 Influence of dissolved oxygen in the reaction solution

As nanoscale zero-valent iron is easily oxidized by oxygen in air or aqueous solution, different dissolved oxygen contents in the reaction solution (0, 2.0, and 4.0 mg/L, respectively) were investigated. As seen from **Fig. 7b**, the removal efficiency for BDE-209 decreased with increasing dissolved oxygen content. After 4 hr, the removal efficiency of BDE-209 was decreased from 98.12% to 78.14% when the dissolved oxygen increased from 0.0 to 4.0 mg/L. With the increase of dissolved oxygen, more nanoscale zero-valent iron particles would be oxidized, and these iron oxides and hydrated oxide products could precipitate on

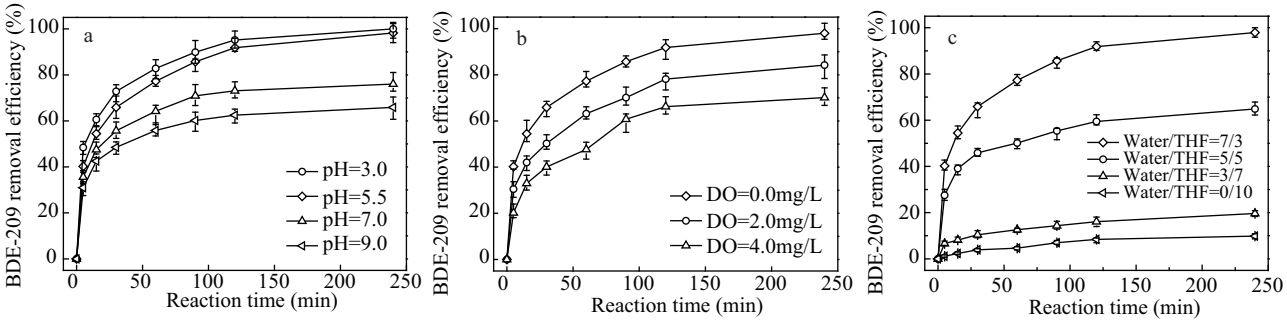

Fig. 7 Effect of different initial pH (a), different initial DO (b), and different solvent conditions (c) on BDE-209 removal. Experimental conditions: initial BDE-209 concentration 2.0 mg/L; material dosage 0.60 g; temperature (25 ± 1)°C, initial pH 5.5 for (b and c).

the surface of M-NZVI (Chen et al., 2011b). The thickness of the iron oxide layer on the surface would be accordingly increased (confirmed by XPS), thus reducing the activity of nanoscale zero-valent iron particles (Keenan et al., 2008) and weakening the electron transfer between the zero-valent iron particles and BDE-209, and finally reducing the removal efficiency of M-NZVI for BDE-209.

Due to its high hydrophobicity, BDE-209 needed to be dissolved in a certain percentage of a co-solvent (THF) before dissolving in water. Different THF/water ratios (THF:water = 3:7, 5:5, 7:3, and 10:0) were conducted to test the influence of solvent on the degradation on BDE-209 (**Fig. 7c**). This showed that as the proportion of THF in the "THF-water" system increased, the removal efficiency of M-NZVI for BDE-209 decreased. After 4 hr of reaction, the removal efficiency on BDE-209 with ratios of THF/water of 3:7, 5:5, 7:3, and 10:0 was 97.92%, 63.86%, 19.64%, and 1.05%, respectively, which was consistent with others' results (Fang et al., 2011b). The main reason was that the process of debromination required a certain amount of hydrogen ions (Shih et al., 2010; Li et al., 2007), and the hydrogen ions could be obtained from the water, as the dissociation constant of water was much larger than that of pure THF (Fang et al., 2011b). Therefore, the more hydrogen ions the reaction solution could provide, the better debromination would be obtained. However, the proportion of water in the "THF-water" system could not be too high since the BDE-209 solid must be completely dissolved in the "THF-water" system. In this experiment, the THF/water ratio of 3:7 was relatively satisfactory.

3 Conclusions

In this study, organo-montmorillonite, as a good carrier and dispersant, could immobilize nanoscale zero-valent iron, which was formed on the organo-montmorillonite by a liquid phase reduction reaction. The characterization results of XRD, SEM, TEM, and XPS showed that nanoscale zero-valent iron having a core-shell structure had good dispersion on the organo-montmorillonite. The presence of organo-montmorillonite could greatly enhance the reduction activity of nanoscale zero-valent iron, and the removal efficiency of M-NZVI for BDE-209 was much higher than that of NZVI. The removal efficiency of M-NZVI for BDE-209 decreased with increasing pH and initial dissolved oxygen content in the reaction solution, but increased with increasing proportion of water.

Acknowledgments

This work was supported by the National Science and Technology Major Projects of Water Pollution Control and Management of China (No. 2012ZX07206002).

REFERENCES

An, T.C., Chen, J.X., Li, G.Y., Ding, X.J., Sheng, G.Y., Fu, J.M. et al., 2008. Characterization and the photocatalytic activity of TiO_2 immobilized hydrophobic montmorillonite photocatalysts degradation of decabromodiphenyl ether (BDE-209). Catal. Today 139, 69–76.

Chen, J.W., Xiu, Z.M., Lowry, G.V., Alvarez, P.J.J., 2011a. Effect of natural organic matter on toxicity and reactivity of nano-scale zero-valent iron. Water Res. 45, 1995–2001.

Chen, Z.X., Jin, X.Y., Chen, Z.L., Megharaj, M., Naidu, R., 2011b. Removal of methyl orange from aqueous solution using bentonite-supported nanoscale zero-valent iron. J. Coll. Int. Sci. 363, 601–607.

Crane, R.A., Scott, T.B., 2012. Nanoscale zero-valent iron: future prospects for an emerging water treatment technology. J. Hazard. Mater. 211-212, 112–125.

Dong, J., Zhao, Y.H., Zhao, R., Zhou, R., 2010. Effects of pH and particle size on kinetics of nitrobenzene reduction by zero-valent iron. J. Environ. Sci. 22, 1741–1747.

Dorathi, P.J., Kandasamy, P., 2012. Dechlorination of chlorophenols by zero valent iron impregnated silica. J. Environ. Sci. 24, 765–773.

Fang, M.D., Yuan, P., Chen, T.H., He, H.P., Yuan, A.H., Chen, K.M. et al., 2010. Synthesis, characterization and size control of zerovalent iron nanoparticles anchored on m ontmorillonite. Chin. Sci. Bull. 55, 1092–1099.

Fang, Z.Q., Qiu, X.H., Chen, J.H., Qiu, X.Q., 2011a. Debromination of polybrominated diphenyl ethers by Ni/Fe bimetallic nanoparticles: influencing factors, kinetics, and mechanism. J. Hazard. Mater. 185, 958–969.

Fang, Z.Q., Qiu, X.H., Chen, J.H., Qiu, X.Q., 2011b. Degradation of the polybrominated diphenyl ethers by nanoscale zero-valent metallic particles prepared from steel pickling waste liquor. Desalination 267, 34–41.

Gu, C., Jia, H.Z., Li, H., Teppen, B.J., Boyd, S.A., 2010. Synthesis of highly reactive subnano-sized zero-valent iron using smectite clay templates. Environ. Sci. Technol. 44, 4258–4263.

He, J., Robrock, K.R., Alvarez-Cohen, L., 2006. Microbial reductive debromination of polybrominated diphenyl ethers (PBDEs). Environ. Sci. Technol. 40, 4429–4434.

He, Y., Gao, J.F., Feng, F.Q., Liu, C., Peng, Y.Z., Wang, S.Y., 2012. The comparative study on the rapid decolorization of azo, anthraquinone and triphenylmethane dyes by zero-valent iron. Chem. Eng. J. 179, 8–18.

Jia, H.Z., Wang, C.Y., 2012. Adsorption and dechlorination of 2, 4-dichlorophenol (2,4-DCP) on a multi-functional organo-smectite templated zero-valent iron composite. Chem. Eng. J. 191, 202–209.

Kanel, S.R., Manning, B., Charlet, L., Choi, H., 2005. Removal of arsenic (III) from groundwater by nanoscale zero-valent iron. Environ. Sci. Technol. 39, 1291–1298.

Keenan, C.R., Sedlak, D.L., 2008. Factors affecting the yield of oxidants from the reaction of nanoparticulate zero-valent iron and oxygen. Environ. Sci. Technol. 42, 1262–1267.

Keum, Y.S., Li, Q.X., 2005. Reductive debromination of polybrominated diphenyl ethers by zerovalent iron. Environ. Sci. Technol. 39, 2280–2286.

Kim, J.H., Tratnyek, P.G., Chang, Y.S., 2008. Rapid dechlorination of polychlorinated dibenzo-p-dioxins by bimetallic and nanosized zerovalent iron. Environ. Sci. Technol. 42, 4106–4112.

Law, K., Halldorson, T., Danell, R., Stern, G., Gewurtz, S., Alaee, M. et al., 2006. Bioaccumulation and trophic transfer of some brominated flame retardants in a Lake Winnipeg (Canada) food web. Environ. Toxicol. Chem. 25, 1283–1290.

Lee, S.H., Lee, K.H., Rhee, S.S., Park, J.B., 2007. Development of a new zero-valent iron zeolite material to reduce nitrate without ammonium release. J. Environ. Eng. 133, 6–12.

Li, A., Tai, C., Zhao, Z.S., Wang, Y.W., Zhang, Q.H., Jiang, G.B. et al., 2007. Debromination of decabrominated diphenyl ether by resin-bound iron nanoparticles. Environ. Sci. Technol. 41, 6841–6846.

Li, L., Fan, M.H., Brown, R.C., Leeuwen, J.V., Wang, J.J., Wang, W.H. et al., 2006. Synthesis, properties, and environmental applications of nanoscale iron-based materials: A Review. Crit. Rev. Environ. Sci. Technol. 36, 405–431.

Li, X.Q., Zhang, W.X., 2006. Iron nanoparti cles: the core-shell structure and unique properties for Ni(II) sequestration. Langmuir 22, 4638–4642.

Li, Y.M., Zhang, Y., Li, J.F., Zheng, X.M., 2011. Enhanced removal of pentachlorophenol by a novel composite: nanoscale zero valent iron immobilized on organobentonite. Environ. Pollut. 159, 3744–3749.

Liu, Y.Q., Lowry, G.V., 2006. Effect of particle age (Fe^0 content) and solution pH on NZVI reactivity: H_2 evolution and TCE dechlorination. Environ. Sci. Technol. 40, 6085–6090.

Lowry, G.V., Johnson, K.M., 2004. Congener-specific dechlorination of dissolved PCBs by microscale and nanoscale zero valent iron in a water/methanol solution. Environ. Sci. Technol. 38, 5208–5216.

Luo, Y., Luo, X.J., Lin, Z., Chen, S.J., Liu, J., Mai, B.X. et al., 2009. Polybrominated diphenyl ethers in road and farmland soils from an e-waste recycling region in Southern China: concentrations, source profiles, and potential dispersion and deposition. Sci. Total Environ. 407, 1105–1113.

Martin, J.E., Herzing, A.A., Yan, W.L., Li, X.Q., Koel, B.E., Kiely, C. J. et al., 2008. Determination of the oxide layer thickness in core-shell zerovalent iron nanoparticles. Langmuir 24, 4329–4334.

Qiu, X.Q., Fang, Z.Q., Liang, B., Gu, F.L., Xu, Z.C., 2011. Degradation of decabromodiphenyl ether by nano zero-valent iron immobilized in mesoporous silica microspheres. J. Hazard. Mater. 193, 70–81.

Schoonheydt, R.A., 2002. Smectite-type clay minerals as nanomaterials. Clays Clay Miner. 50, 411–420.

Shahwan, T., Üzüm, Ç., Eroğlu, A. E., Lieberwirth, I., 2010. Synthesis and characterization of bentonite/iron nanoparticles and their application as adsorbent of cobalt ions. Appl. Clay Sci. 47, 257–262.

Shakir, K., Ghoneimy, F.H., Elkafrawy, A.F., Beheir, S.G., Refaat, M., 2008. Removal of catechol from aqueous solutions by adsorption onto organophilic-bentonite. J. Hazard. Mater. 150, 765–773.

Shi, L.N., Zhang, X., Chen, Z.L., 2011. Removal of chromium(VI) from wastewater using bentonite-supported nanoscale zero-valent iron. Water Res. 45, 886–892.

Shih, Y.H., Chen, Y.C., Chen, M.Y., Tai, Y.T., Tso, C.P., 2009. Dechlorination of hexachlorobenzene by using nanoscale Fe and nanoscale Pd/Fe bimetallic particles. Coll. Sur. A-Physicochem. Eng. Aspects 332, 84–89.

Shih, Y.H., Tai, Y.T., 2010. Reaction of decabrominated diphenyl ether by zerovalent iron nanoparticles. Chemosphere 78, 1200–1206.

Sun, Y.P., Li, X.Q., Cao, J.S., Zhang, W.X., Wang, H.P., 2006. Characterization of zero-valent iron nanoparticles. Adv. Colloid Interface Sci. 120, 47–56.

Üzüm, C., Shahwan, T., Eroglu, A.E., Hallam, K.R., Scott, T.B., Lieberwirth, I., 2009. Synthesis and characterization of kaolinite-supported zero-valent iron nanoparticles and their application for the removal of aqueous Cu^{2+} and Co^{2+} ions. Appl. Clay Sci. 43, 172–181.

Üzüm, C., Shahwan, T., Eroglu, A.E., Lieberwirth, I., Scott, T.B., Hallam, K. R., 2008. Application of zero-valent iron nanoparticles for the removal of aqueous Co^{2+} ions under various experimental conditions. Chem. Eng. J. 144, 213–220.

Xu, J.H., Gao, N.Y., Tang, Y.L., Deng, Y., Sui, M.H., 2010. Perchlorate removal using granular activated carbon supported iron compounds: Synthesis, characterization and reactivity. J. Environ. Sci. 22, 1807–1813.

Yu, K., Gu, C., Boyd, S. A., Liu, C., Sun, C., Teppen, B.J. et al., 2012. Rapid and extensive debromination of decabromodiphenyl ether by smectite clay-templated subnanoscale zero-valent iron. Environ. Sci. Technol. 46, 8969–8975.

Zhan, J.J., Zheng, T.H., Piringer, G., Day, C., McPherson, G.L., Lu, Y.F. et al., 2008. Transport characteristics of nanoscale functional zerovalent iron/silica composites for in situ remediation of trichloroethylene. Environ. Sci. Technol. 42, 8871–8876.

Zhang, X., Lin, S., Chen, Z.L., Megharaj, M., Naidu, R., 2011a. Kaolinite-supported nanoscale zero-valent iron for removal of Pb^{2+} from aqueous solution: reactivity, characterization and mechanism. Water Res. 45, 3481–3488.

Zhang, Y., Li, Y.M., Zheng, X.M., 2011b. Removal of atrazine by nanoscale zero valent iron supported on organobentonite. Sci. Total Environ. 409, 625–630.

Zhang, Z., Cissoko, N., Wo, J.J., Xu, X.H., 2009. Factors influencing the dechlorination of 2,4-dichlorophenol by Ni-Fe nanoparticles in the presence of humic acid. J. Hazard. Mater. 165, 78–86.

Zhao, H.X., Zhang, F.F., Qu, B. C., Xue, X.Y., Liang, X.M., 2009. Wet air co-oxidation of decabromodiphenyl ether (BDE-209) and tetrahydrofuran. J. Hazard. Mater. 169, 1146–1149.

Zhu, L. Z., Li, Y.M., Zhang, J.Y., 1997. Sorption of organobentonites to some organic pollutants in water. Environ. Sci. Technol. 31, 1407–1410.

Zhuang, Y., Ahn, S.W., Luthy, R. G., 2010. Debromination of polybrominated diphenyl ethers by nanoscale zerovalent iron: pathways, kinetics, and reactivity. Environ. Sci. Technol. 44, 8236–8242.

Zhuang, Y., Ahn, S.W., Seyfferth, A.L., Masue-Slowey, Y., Fendorf, S., Luthy, R.G., 2011. Dehalogenation of polybrominated diphenyl ethers and polychlorinated biphenyl by bimetallic, impregnated, and nanoscale zerovalent iron. Environ. Sci. Technol. 45, 4896–4903.

Editorial Board of Journal of Environmental Sciences

JOURNAL OF ENVIRONMENTAL SCIENCES

环境科学学报(英文版)

(http://www.jesc.ac.cn)

Aims and scope

Journal of Environmental Sciences is an international academic journal supervised by Research Center for Eco-Environmental Sciences, Chinese Academy of Sciences. The journal publishes original, peer-reviewed innovative research and valuable findings in environmental sciences. The types of articles published are research article, critical review, rapid communications, and special issues.

The scope of the journal embraces the treatment processes for natural groundwater, municipal, agricultural and industrial water and wastewaters; physical and chemical methods for limitation of pollutants emission into the atmospheric environment; chemical and biological and phytoremediation of contaminated soil; fate and transport of pollutants in environments; toxicological effects of terrorist chemical release on the natural environment and human health; development of environmental catalysts and materials.

For subscription to electronic edition

Elsevier is responsible for subscription of the journal. Please subscribe to the journal via http://www.elsevier.com/locate/jes.

For subscription to print edition

China: Please contact the customer service, Science Press, 16 Donghuangchenggen North Street, Beijing 100717, China. Tel: +86-10-64017032; E-mail: journal@mail.sciencep.com, or the local post office throughout China (domestic postcode: 2-580).

Outside China: Please order the journal from the Elsevier Customer Service Department at the Regional Sales Office nearest you.

Submission declaration

Submission of an article implies that the work described has not been published previously (except in the form of an abstract or as part of a published lecture or academic thesis), that it is not under consideration for publication elsewhere. The submission should be approved by all authors and tacitly or explicitly by the responsible authorities where the work was carried out. If the manuscript accepted, it will not be published elsewhere in the same form, in English or in any other language, including electronically without the written consent of the copyright-holder.

Submission declaration

Submission of the work described has not been published previously (except in the form of an abstract or as part of a published lecture or academic thesis), that it is not under consideration for publication elsewhere. The publication should be approved by all authors and tacitly or explicitly by the responsible authorities where the work was carried out. If the manuscript accepted, it will not be published elsewhere in the same form, in English or in any other language, including electronically without the written consent of the copyright-holder.

Editorial

Authors should submit manuscript online at http://www.jesc.ac.cn. In case of queries, please contact editorial office, Tel: +86-10-62920553, E-mail: jesc@263.net, jesc@rcees.ac.cn. Instruction to authors is available at http://www.jesc.ac.cn.

Journal of Environmental Sciences (Established in 1989)

Vol. 26 No. 2 2014

Supervised by	Chinese Academy of Sciences	**Published by**	Science Press, Beijing, China
Sponsored by	Research Center for Eco-Environmental		Elsevier Limited, The Netherlands
	Sciences, Chinese Academy of Sciences	**Distributed by**	
Edited by	Editorial Office of Journal of	Domestic	Science Press, 16 Donghuangchenggen
	Environmental Sciences		North Street, Beijing 100717, China
	P. O. Box 2871, Beijing 100085, China		Local Post Offices through China
	Tel: 86-10-62920553; http://www.jesc.ac.cn	Foreign	Elsevier Limited
	E-mail: jesc@263.net, jesc@rcees.ac.cn		http://www.elsevier.com/locate/jes
Editor-in-chief	Hongxiao Tang	**Printed by**	Beijing Beilin Printing House, 100083, China

CN 11-2629/X **Domestic postcode: 2-580** **Domestic price per issue RMB ¥ 110.00**

ISSN 1001-0742